Relational Clocks in a Quantum Ledger

Construction, Preparation and the Limits of Energy Universality

David Elliman

10 November 2026
Research preprint, version 1.0

Abstract

A stationary quantum state can describe change through correlations between a clock and the system it measures. This observation leaves a constructive question: can elementary exchanges with a reservoir supply the clock's energies, its correlations and its response to other records, rather than having each ingredient specified separately? We investigate finite quantum registers whose interactions are reversible transactions, without assigning them positions or a spatial geometry. A vacancy counterpart of a three-record rule produces complementary clock energies, and a matching exchange selects the correlated state above a calculable threshold. Selection does not imply preparation: closed evolution preserves the target population, and a conserved symmetry blocks preparation by the tested finite receiving bank for initially definite record words. A modified interaction exports that symmetry label and prepares the clock conditionally in a cold continuous-reservoir limit, with explicit energy and memory accounting. A configuration-normalised storage rule gives a truncated bosonic ladder. Coupling that ladder to free records produces a stationary second-order frequency response exactly proportional to record energy; its sign depends on the bank quantum. The tested interacting records violate this proportionality, and the native clock can distinguish states of equal energy. These constructions identify a missing transaction-strength sum rule, rather than deriving universal gravitational coupling. Quantum mechanics, Hamiltonian ordering and the stated reservoir resources remain assumptions; spacetime and particle masses are not derived.

Contents

1 Introduction 3

2 Records and reversible transactions 4

3 Finite conditional clocks 5

4 A clock from the vacancy counterpart 8

5 Preparation: energy, symmetry and retained information 9

6 Coherent storage and its response 15

7 Response to the full transaction energy 16

8 Testing the counterpart clock itself 20

9 Relation to prior work and the remaining problem 21

10 Conclusions 22

A Spectrum of the three-record module 23

B Resonances and the order of the response 24

C Reproducibility, corrections and claim provenance 25

1 Introduction

A clock is a physical system whose changing state lets us label changes in another system. Usually we give both systems an external time parameter and then ask how accurately one tracks the other. The Page–Wootters construction asks a different question: can a joint state that is stationary as a whole contain correlations that look like evolution when one subsystem is read as a clock? The answer is yes, provided its energies and correlations have the appropriate structure [1, 2]. That structure is mathematically well understood. Explaining why a proposed underlying system would possess it is a separate problem.

This paper approaches that problem through a deliberately small model. A *record* is a quantum register, a *bank* is an additional register that can accept and return resources, and a *transaction* is a Hermitian coupling between specified register states. These terms provide an accounting language for ordinary quantum mechanics. They do not assume that nature executes software, and they do not identify a register with an observed particle. The broader motivation is to ask whether a common microscopic rule could eventually account for several effective physical features. Here the question is restricted to clocks and their response to energy.

No position, distance, spatial dimension, metric or lattice is assigned to a register. Labels distinguish kinds of transaction and energy denominations. Their algebraic relations are supplied explicitly. Hilbert spaces and inner products are assumed; the absence of *spatial* geometry does not mean the absence of mathematical structure. A mapping from this description to observations in spacetime remains an open part of the programme.

Five questions must be separated. Does the clock have compatible energies? Is the correctly correlated state energetically selected? Can the dynamics prepare it from declared initial resources? Can an observer read it with the measurement costs included? Does its response to another system depend universally on that system's total energy? A success at one step need not imply success at the next. The constructions below provide explicit examples of these distinctions.

The positive results are a complementary-spectrum identity, an exchange-selected correlated state, conditional preparation in a reservoir limit, a finite storage ladder and an energy-proportional stationary response for free records. The limitations are equally informative. The simplest common-strength exchange does not select the desired clock; a closed action cannot attract states into its own exact eigenstate; an energy-receiving bank can leave a relevant symmetry label trapped; and the tested transaction couplings do not respond universally to interacting-record energy. One counterexample uses two states with identical energy and packet-count statistics but opposite clock shifts.

The contribution is this explicit, reproducible chain of constructions and counterexamples. Conditional time, entangled parent Hamiltonians, collective storage amplitudes and dispersive elimination are established methods, and we identify the corresponding prior art. We make no priority claim for those methods and no empirical claim that the model describes the physical vacuum.

1.1 What is assumed and what is established

Table 1 summarises the logical dependencies. In particular, the counterpart clock, the reservoir used for preparation and the occupation probe used for response are distinct tested constructions. We have not found one interaction that accomplishes all their tasks together.

We use $\hbar = 1$ and set the primitive internal transaction strength to one. Energies and all numerical parameters are therefore dimensionless. The symbol u denotes the ordering parameter of a supplied Hamiltonian evolution used to test the model. The symbol t labels a clock reading. A conditional state varying with t does not eliminate the assumed Hamiltonian law or derive

Question	Supplied structure	Consequence and remaining limitation
Compatible clock	Vacancy counterpart with matched real strengths	Complementary energies follow algebraically; the counterpart rule is not derived.
Correlated state	Positive matching exchange of strength J	The state is selected above J_*; the hierarchy is an input.
Preparation	Symmetry-exporting read, cold continuous bank, weak-coupling limit	The tested limit generators converge to the ground state; finite autonomous preparation is open.
Storage	Coherent any-order access, normalisation per occupied configuration	Truncated bosonic matrix elements follow; neither Bose statistics nor the budget law is derived.
Energy response	Shared transaction coupling and a specified dressed probe	Free stationary response is proportional to energy at second order; tested interacting modules fail.
Spacetime interpretation	None supplied	No distance, gravitational field, equivalence principle or particle spectrum is established.

Table 1: Assumptions and results. A mathematical implication is conditional on the entries in the middle column.

every meaning of physical time. The slow reservoir parameter is $\tau = \eta^2 u$, where η is its coupling strength.

The principal mirror model fixes $\lambda = 1$ and has one continuous ratio, J. Its cold preparation extension adds η and Λ. The occupation-probe family has three continuous inputs, λ, ω, g, and integer capacity d. Finite-clock bandwidth, reference energy, capacity and measurement choices are declared benchmark resources. None is estimated from empirical data.

Notation at a glance

t	Conditional clock reading.
u	Supplied Hamiltonian ordering parameter used in dynamical tests.
$\tau = \eta^2 u$	Slow parameter held fixed in the weak-coupling reservoir limit.
J, λ	Matching-exchange strength; strength of the gated internal transaction.
ω, ϖ	Bank packet spacing; Bohr energy difference in the cold-bank generator.
g, η	Occupation-probe coupling; cold preparation-bank coupling.
d, d_C	Occupation-bank capacity; number of levels in the supplied finite clock.
Λ	Cold-bank spectral scale; the cited model in §9 separately uses this symbol for its interaction scale.

Sections 2–4 construct the records and clocks. Section 5 treats preparation and resource accounting. Sections 6–8 derive and compare two response mechanisms. Section 9 locates the results in the literature and states the remaining physical problem. Appendices give the finite spectrum, resonant corrections and the evidence map.

2 Records and reversible transactions

2.1 The elementary rule

For two allowed joint configurations i and f, a transaction has the form

$$h_{if} = g_{if}|f\rangle\langle i| + g_{if}^*|i\rangle\langle f|. \tag{1}$$

Its reverse is part of the same operator. A conserved label Q must satisfy $[H, Q] = 0$ for the complete Hamiltonian. A reversible interaction preserves inner products of complete states. Returning a counter to its original value is weaker than returning all auxiliary quantum information: an unobserved route register can still retain correlations.

For a time-independent closed model, $U(u) = e^{-iHu}$ is unitary and the full energy is conserved. The separate energies of a record, a bank and their interaction need not be conserved. This distinction matters in every preparation calculation below. We do not permit an omitted reverse term or a silently reset memory to serve as an absorber.

2.2 A small interacting module

Consider three binary record labels $j = 0, 1, 2$, with

$$l_j = |0\rangle\langle 1|_j, \qquad n_j = l_j^\dagger l_j, \qquad X_j = l_j + l_j^\dagger, \qquad Z_j = \mathbb{I} - 2n_j. \tag{2}$$

They are transaction types, not directions. A basis word w also carries a counter $q = 3 - |w|$, where $|w|$ counts occupied labels. The notation $|w\rangle$ abbreviates the injective encoding $|q = 3 - |w|\rangle|w\rangle$. Thus an eight-dimensional physical sector retains both word and counter. Tracing out the counter would remove coherence between different word counts and would define a different subsystem.

The declared module is

$$\begin{aligned} L_\lambda &= l_0 + l_1 + \lambda n_0 n_1 l_2, \\ H_S &= 3\mathbb{I} + A_S, \qquad A_S = L_\lambda + L_\lambda^\dagger = X_0 + X_1 + \lambda n_0 n_1 X_2. \end{aligned} \tag{3}$$

The third transaction requires the first two records to be occupied. The gate is the model's specified interaction between records; it is not a derived force or a demonstration of a bound physical particle. The main case is $\lambda = 1$. Comparisons use $\lambda = 0, 1/2$, and an explicitly ungated three-transaction module.

The counter explains which resource sectors are retained, but its numerical value is not the interacting energy. For example, the $\lambda = 1$ spectrum is

$$\operatorname{spec} H_S \simeq \{0.657077, 1.186393, 2.529317, 3, 3, 3.470683, 4.813607, 5.342923\}. \tag{4}$$

These values follow from the specified transaction matrix. They are not measured particle energies. Appendix A derives its characteristic polynomial.

All phases in this paper follow from a declared Hermitian operator, an explicitly stated input state or a measurement convention. In particular, the alternating signs of the correlated clock state below follow from positive exchange. No phase or energy value is chosen to fit a mass ratio or gravitational observation.

3 Finite conditional clocks

3.1 An exact energy-shell construction

Let $H_S = \sum_a E_a P_a$, where P_a projects onto a distinct energy, including its full degeneracy. Give an additional clock one state $|a\rangle_C$ at energy $E_* - E_a$. For a normalised input $|\psi\rangle$, define

$$|\Psi\rangle = \sum_a |a\rangle_C P_a |\psi\rangle_S, \qquad (H_C + H_S)|\Psi\rangle = E_*|\Psi\rangle. \tag{5}$$

The state is normalised because the P_a are orthogonal. If r is the number of distinct energies, the normalised clock states

$$|t\rangle_C = r^{-1/2} \sum_a e^{-i(E_* - E_a)t} |a\rangle_C \tag{6}$$

give

$${}_C\langle t|\Psi\rangle = r^{-1/2} e^{iE_* t} e^{-iH_S t} |\psi\rangle. \tag{7}$$

The global state changes only by an overall phase under its free joint Hamiltonian, while conditional record states follow the Schrödinger evolution. This is the familiar Page–Wootters mechanism [1–3]. Equation (5) also exposes the input: the clock spectrum has been chosen to complement the system's energies.

Finite clock states at arbitrary labels t need not be orthogonal. For m chosen readings, a simple valid positive-operator-valued measure (POVM) is

$$E_k = \frac{1}{m} |t_k\rangle\langle t_k|, \qquad E_{\text{fail}} = \mathbb{I} - \sum_{k=1}^{m} E_k \geq 0. \tag{8}$$

Positivity follows because every rank-one projector is at most $\mathbb{I}$. Each specified reading of (5) has probability $1/(mr)$; total success is $1/r$. For the seven distinct energies in (4), the failure probability of this particular POVM is $6/7$. This is an inefficient normalisation choice, not a fundamental limitation on all clock measurements. More efficient finite-clock constructions and autonomous clocks have their own hypotheses and resource bounds [4, 5].

The reading effects and initial seed are specified apparatus. Conditioning is not a physical procedure that prepares an arbitrary unknown input for free. In a sequential measurement calculation, apparatus records must also be retained. With two projective writes P_a, P_b, their joint probability is

$$p(a, b) = \| P_b e^{-iH_S(t_2 - t_1)} P_a e^{-iH_S t_1} \psi \|^2. \tag{9}$$

This follows by coherently writing each outcome into its own memory and taking the final joint Born probabilities. Reading a free clock twice without those writes is not the same experiment [2].

3.2 An equally spaced clock: accuracy and stationarity

A simpler spectrum illustrates why capacity alone is insufficient. Let a clock have d_C levels,

$$H_C = \delta \sum_{n=0}^{d_C - 1} n |n\rangle\langle n|, \qquad \delta = \frac{B}{d_C}. \tag{10}$$

Here B is the fixed spectral-window scale; the highest clock energy is $B - \delta$. Choose the nearest integer

$$n_a = \left\lfloor \frac{E_* - E_a}{\delta} + \tfrac{1}{2} \right\rfloor, \qquad \widetilde{E}_a = E_* - \delta n_a. \tag{11}$$

Retain only $0 \leq n_a < d_C$. With $p_{\text{keep}} = \sum_{a\,\text{retained}} \|P_a \psi\|^2$, the corresponding joint state is

$$|\widetilde{\Psi}\rangle = \frac{1}{\sqrt{p_{\text{keep}}}} \sum_{a\,\text{retained}} |n_a\rangle P_a |\psi\rangle. \tag{12}$$

Its conditional state evolves exactly under $\widetilde{H}_S = \sum_a \widetilde{E}_a P_a$, rather than exactly under the unchanged physical H_S. On retained components,

$$|\widetilde{E}_a - E_a| \leq \delta/2, \qquad \|(H_C + H_S - E_*)\widetilde{\Psi}\|^2 = \frac{\sum_a \|P_a \psi\|^2 (E_a - \widetilde{E}_a)^2}{p_{\text{keep}}}. \tag{13}$$

d_C	Minimum sampled state fidelity	Minimum process fidelity
8	0.132345	0.359716
16	0.743005	0.860187
32	0.944692	0.967053
64	0.975624	0.986121
128	0.992395	0.995601
256	0.999975655	0.999986069

Table 2: Fixed-window comparison for the equally spaced clock. These are finite numerical benchmarks of a supplied clock, not observed physical accuracies.

Different residuals on occupied components mean that the joint pure state is not exactly stationary. Its mean total energy is nevertheless conserved by the time-independent joint Hamiltonian. Conservation and stationarity are different requirements.

For full retained support, the commuting spectral representation gives

$$\|e^{-i\widetilde{H}_S t} - e^{-iH_S t}\| \le |t|\delta/2, \qquad 1 - F(t) \le \min\{1, t^2\delta^2/4\}, \tag{14}$$

where F is squared pure-state fidelity. The operator bound follows from $|e^{-ix} - e^{-iy}| \le |x - y|$; the fidelity bound follows by applying it to a normalised state. It also applies to the process state obtained by adjoining an unchanged reference.

Orthogonal Fourier readings have spacing and period

$$\Delta t = \frac{2\pi}{d_C\delta} = \frac{2\pi}{B}, \qquad T = \frac{2\pi}{\delta} = \frac{2\pi d_C}{B}. \tag{15}$$

Increasing capacity at fixed B refines the energy resolution and extends the period. It does not refine the native reading interval. Equation (14) gives a shrinking error envelope on a fixed interval, not on an interval growing like T.

For $B = 8$, $E_* = 7$ and the frozen module (3), 11 declared inputs were compared at five readings $0, \pi/4, \ldots, \pi$. Table 2 reports saved results. The especially accurate last row reflects rounding of this particular spectrum. It is not a universal threshold. The minimum full-period process fidelity instead changes from approximately 3.36×10^{-5} at $d_C = 128$ to 0.944700 at $d_C = 256$; full-period convergence was not established.

If the spectral window excludes part of the input, conditioning and renormalising do not recover it: at $t = 0$, fidelity to the intended input is p_{keep}, even when fidelity to its normalised projection is one. Nor does counting repeated periods supply an unlimited clock for free. A cycle record is additional memory. The gauge-invariance issues for periodic relational clocks require particular care [6]; the present diagnostic labels do not establish a global monotonic observable.

Finally, the original counter is not already the required clock. In a sector $q + N_S = 3$, conditioning its phase state gives

$$\langle\theta|\Psi\rangle = e^{3i\theta}e^{-iN_S\theta}\langle 0|\Psi\rangle. \tag{16}$$

This reads word count $N_S = \sum_j n_j$, not the transaction Hamiltonian. The distinction motivates a clock with its own internal transactions.

4 A clock from the vacancy counterpart

4.1 Complementary energies from an operator identity

Use the same elementary strengths on vacant, rather than occupied, prerequisites:

$$H_C = 3\mathbb{I} + A_C, \qquad A_C = X_0 + X_1 + \lambda(\mathbb{I} - n_0)(\mathbb{I} - n_1)X_2. \tag{17}$$

Let F complement all three bits and $P = (-1)^{N_S}$ be word parity. Every term of A_S flips exactly one bit, so

$$PA_SP = -A_S, \qquad A_C = FA_SF, \qquad R = FP. \tag{18}$$

The matrices are real and symmetric. Consequently

$$H_C R + R H_S^T = 6R. \tag{19}$$

For example, $A_C R = FA_SP = -FPA_S = -RA_S$. Thus if $H_S|e\rangle = E|e\rangle$, then $R|e^*\rangle$ has clock energy $6 - E$. The clock matrix was constructed from the rule, not from a list of eigenvalues. The supplied vacancy relation and matched strengths are precisely what make this possible.

The derivation extends to arbitrary real strengths of the three terms when the corresponding strengths agree between modules. It also extends to a real, parity-odd transaction matrix on more bits with its bit-complement counterpart. It does not show why a physical bank must implement that counterpart.

4.2 Exchange selects the correlated state

Couple corresponding labels through

$$V = \sum_{j=0}^{2} (l_{Cj}^\dagger l_{Sj} + l_{Cj} l_{Sj}^\dagger), \qquad H_Q = H_C \otimes \mathbb{I} + \mathbb{I} \otimes H_S + JV, \tag{20}$$

with $J > 0$. Both module counters adjust within their encoded physical sectors. Define

$$|\Omega\rangle = \frac{1}{\sqrt{8}} \sum_w (-1)^{|w|} |\bar{w}\rangle_C |w\rangle_S = (R \otimes \mathbb{I})|\Phi_8\rangle, \qquad |\Phi_8\rangle = \frac{1}{\sqrt{8}} \sum_w |w\rangle|w\rangle. \tag{21}$$

For each corresponding pair, positive exchange has an antisymmetric eigenvector with eigenvalue -1. Their product is (21), up to an irrelevant overall sign. Equation (19) and the identity $(A \otimes \mathbb{I}) \operatorname{vec} R = \operatorname{vec}(AR)$ imply

$$(H_C + H_S)|\Omega\rangle = 6|\Omega\rangle, \qquad V|\Omega\rangle = -3|\Omega\rangle, \qquad H_Q|\Omega\rangle = (6 - 3J)|\Omega\rangle. \tag{22}$$

The reduced state of either module is $\mathbb{I}_8/8$, with entropy three bits. This is a mirror-transformed maximally entangled state, equivalent in entanglement structure to the infinite-temperature thermofield double. General constructions of entangled parent Hamiltonians are established prior art [7]; the complementary energies and transaction gates here specify a particular example.

Proposition 4.1 (Conditional ground-state selection)**.** *For $\lambda = 1$, $J > 6$ suffices to make $|\Omega\rangle$ the unique ground state of H_Q. The exact transition is determined by a finite generalised eigenvalue problem and is numerically $J_* = 1.5235318058\ldots$ in the chosen units.*

Proof. On $|\Omega\rangle^\perp$, $D = V + 3\mathbb{I}$ is strictly positive with smallest eigenvalue one. Write $A = A_C \otimes \mathbb{I} + \mathbb{I} \otimes A_S$. It annihilates $|\Omega\rangle$, and $\|A\| \le 6$. Thus $H_Q - (6 - 3J)\mathbb{I} = A + JD \ge (J - 6)\mathbb{I}$ on

that complement. More precisely, congruence by $D^{-1/2}$ shows that strict positivity is equivalent to

$$J > J_* = -\lambda_{\min}\Big(D^{-1/2} A D^{-1/2}\big|_{|\Omega\rangle^\perp}\Big). \tag{23}$$

This gives both the threshold and uniqueness above it. The quoted value was checked by this construction and by a separate level-crossing bisection. □

At $J = 1$ the proposed state has energy three, whereas the actual ground energy is approximately 1.708059. The common-strength model therefore fails to select it. At $J = 2$ and 8 it is the ground state, with gaps approximately 0.673318 and 7.490168. The $J = 2$ value comes from the banked M3b rerun of this same action; PW2 itself sampled $J = 0, 1, 8$. These are open-range selection results, not a fit of individual energy levels; the reason for the hierarchy $J > J_*$ remains an input.

4.3 Conditional reading and the preparation obstruction

For a normalised declared seed $|\psi\rangle$, take

$$|c(t)\rangle = e^{-iH_C t} R|\psi^*\rangle. \tag{24}$$

Using (19), contraction with (21) gives

$${}_C\langle c(t)|\Omega\rangle = \frac{e^{6it}}{\sqrt{8}} e^{-iH_S t}|\psi\rangle. \tag{25}$$

A five-effect POVM normalised as in (8) has probability 1/40 per specified reading and total success 1/8. Better measurement families are possible. For a single rank-one time-covariant orbit, degeneracy limits how much of the clock it covers; a bound based on the number of distinct energies applies to that family, not to every possible measurement. Additional seeds and a degeneracy label change the apparatus.

Changing the seed in (25) steers the conditional record input. This is an explicitly supplied readout, not autonomous access to an unknown state. Moreover, energetic selection does not supply a preparation process:

$$[H_Q, |\Omega\rangle\langle\Omega|] = 0 \quad \Longrightarrow \quad \frac{\mathrm{d}}{\mathrm{d}u}\,\mathrm{Tr}[|\Omega\rangle\langle\Omega|\,\rho_Q(u)] = 0. \tag{26}$$

A product input $|c\rangle|s\rangle$ has squared overlap at most 1/8 with a maximally entangled eight-dimensional state, by Cauchy–Schwarz. A separable mixture obeys the same bound by convexity. Evolution under the unchanged closed H_Q cannot increase that target population. This does not forbid entanglement generation or preparation using further resources. It rules out treating its ground-state eigenvector as an attractor of that closed unitary action.

5 Preparation: energy, symmetry and retained information

5.1 Receiving energy is not sufficient

An added bank can change the clock subsystem's target population, since it changes the total action. However, its source operators must connect the required sectors. This can be decided before a large simulation.

For $\lambda = 1$, define the binary symmetry

$$U_Q = X_{C2} X_{S2}. \tag{27}$$

It commutes with H_Q, and $U_Q|\Omega\rangle = -|\Omega\rangle$. The native clock transactions

$$T_0 = X_{C0}, \quad T_1 = X_{C1}, \quad T_2 = (\mathbb{I} - n_{C0})(\mathbb{I} - n_{C1})X_{C2} \tag{28}$$

also commute with U_Q. Therefore any receiving bank coupled only through these T_j preserves the subsystem's U_Q sector weights, whatever the bank's spectrum or capacity.

One explicit finite candidate has a packet register $|n\rangle$, $n = 0, \ldots, L$, and three route-memory bits. Its operators are

$$\begin{aligned}
H_E &= \omega \sum_{n=0}^{L} n|n\rangle\langle n|, & H_M &= \sum_{j=0}^{2} n_{m_j}, \\
B_L &= |s_L\rangle\langle 0| + |0\rangle\langle s_L|, & |s_L\rangle &= L^{-1/2} \sum_{n=1}^{L} |n\rangle, \\
V_E &= \frac{1}{\sqrt{3}} \sum_{j=0}^{2} T_j \otimes B_L \otimes X_{m_j}, & H_{\text{all}} &= H_Q + H_E + H_M + V_E.
\end{aligned} \tag{29}$$

The source norm is bounded as capacity grows, reverse transitions are retained, and a route flag changes on a transfer and changes back on its reversal. The flags retain route parities, not a free chronological history. Increasing L here changes bandwidth as well as dimension.

Proposition 5.1 (Sector obstruction)**.** *If the added interaction commutes with $U_Q \otimes \mathbb{I}_B$, then*

$$F_\Omega(u) \le \operatorname{Tr}\left[\frac{\mathbb{I} - U_Q}{2}\rho_Q(0)\right] \quad \textit{for all } u. \tag{30}$$

For a computational word input this upper bound is $1/2$.

Proof. The projector onto $|\Omega\rangle$ is a subprojector of $P_- = (\mathbb{I} - U_Q)/2$. Conservation of P_- under the full action gives (30). A word state has zero expectation of the simultaneous two-bit flip, so its two symmetry sectors have equal weights. □

In the registered finite test, $J = 1, 2, 8$, $L = 32, 64$ and two packet spacings gave five declared cases and nine word inputs per case. The largest target population in the sampled interval $0 \le u \le 128$ was 0.139062; none satisfied the specified preparation criterion. These finite observations are weaker than the all-time sector bound, but also show that merely reaching that bound was not the issue. The bound was identified after the run began, not predicted in its original registration.

Energy did move into the bank. For one $J = 8$, $L = 32$, $\omega = 1$ input at $u = 128$, the packet and route-memory energies were approximately 4.964916 and 0.647244, while target population remained approximately 0.124481. All five Hamiltonian contributions in (29) sum to the conserved total. The example demonstrates cooling in mean energy without the required state preparation. It excludes this source family and these inputs, not every possible finite bank or every product preparation.

The independent PW3 review also tested four product inputs wholly within the $U_Q = -1$ sector: label 2 was prepared in $|+\rangle_C|-\rangle_S$, with the other two labels complementary. Their sector ceiling is one. Nevertheless, for $J = 8$, $L = 32$, $\omega = 1$ and the same interval $0 \le u \le 128$, their largest sampled target population was approximately 0.233, and their means over the last half of the sampled interval were about 0.16. Removing the sector ceiling therefore did not produce preparation in this finite test. This is evidence that the acceptance dynamics matters as well as symmetry; it is not an all-time impossibility theorem for these inputs.

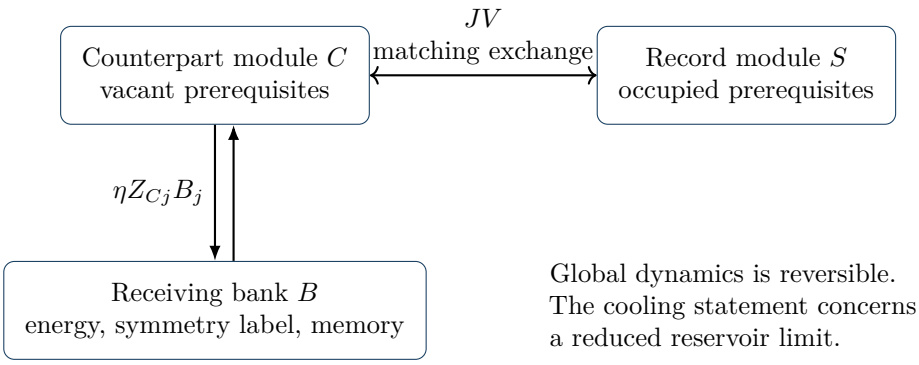


Figure 1: Tensor-factor and interaction schematic for preparation. Placement on the page carries no physical distance or spatial relation. The occupation probe introduced later is a different bank construction.

5.2 A source that exports the label

The next construction changes the source rather than enlarging the same bank. It assumes three distinguishable bosonic packet types with continuous positive energy labels ν:

$$\begin{aligned} H_B &= \sum_{j=0}^{2} \int_0^\infty \nu b_j^\dagger(\nu) b_j(\nu)\, \mathrm{d}\nu, \\ [b_j(\nu), b_k^\dagger(\nu')] &= \delta_{jk}\delta(\nu-\nu'), \\ V_B &= \frac{\eta}{\sqrt{3}} \sum_{j=0}^{2} Z_{Cj} \otimes B_j, \qquad B_j = \int_0^\infty \sqrt{f_\Lambda(\nu)}[b_j(\nu) + b_j^\dagger(\nu)]\, \mathrm{d}\nu, \\ f_\Lambda(\nu) &= \frac{\nu^2 e^{-\nu/\Lambda}}{2\Lambda^3}. \end{aligned} \tag{31}$$

No wavevector or spatial density of states is used. The spectral profile, its scale Λ, the initially empty bank and the coupling η are assumptions. The exponent two is a regular spectral choice, not a derivation of three-dimensional space. Ordinary bosonic reservoir storage is assumed in this preparation model; the finite storage construction in section 6 is a separate result.

The source is an occupation-contrast read. It does not contain a projector onto the target or a prescribed resonant line at a desired clock gap. Since $\int f_\Lambda \mathrm{d}\nu = 1$ and $Z_{Cj}^2 = \mathbb{I}$, the initial vacuum satisfies

$$\langle V_B \rangle = 0, \qquad \langle V_B^2 \rangle = \eta^2 \tag{32}$$

for every clock–record input. The total initial fluctuation budget is therefore independent of that input and of how many energy labels are used to represent the continuum.

Let $U_B = (-1)^{N_2}$ be the parity of type-2 packets. Under U_Q, Z_{C2} changes sign while Z_{C0}, Z_{C1} do not. Under U_B, B_2 changes sign while B_0, B_1 do not. Hence

$$[H_Q + H_B + V_B, U_Q \otimes U_B] = 0, \qquad [V_B, U_Q \otimes \mathbb{I}] \neq 0. \tag{33}$$

A transaction can now change the subsystem's sector while exporting its label to the bank. The globally conserved label is preserved, including superpositions; it is not erased. It is a symmetry of the candidate, not an identified Standard Model charge.

5.3 How the cold response follows from the bank state

The vacuum correlation in the supplied Hamiltonian parameter is

$$\langle B_j(u)B_k(0)\rangle = \delta_{jk}\int_0^\infty f_\Lambda(\nu)e^{-i\nu u}\mathrm{d}\nu = \frac{\delta_{jk}}{(1+i\Lambda u)^3}. \tag{34}$$

The last equality is the elementary gamma integral. Its Fourier transform has support only at positive energy transfer into the bank. This gives the absorption preference: a vacuum mode can receive an emitted packet but contains none to return initially. The microscopic reverse operator is still present.

Assume the weak-coupling, secular reservoir limit, with $\eta \to 0$ at fixed $\tau = \eta^2 u$. This is the setting of quantum Markovian reservoir theory [8]; we analyse the resulting finite generator, without claiming a finite-η convergence bound for the microscopic model. Let P_E be full eigenspace projectors of the *interacting* H_Q. Define

$$A_j(\varpi) = \sum_{E'-E=\varpi} P_E Z_{Cj} P_{E'}, \qquad L_{j\varpi} = \sqrt{\frac{2\pi}{3}f_\Lambda(\varpi)}A_j(\varpi) \quad (\varpi > 0). \tag{35}$$

Equal Bohr frequencies are grouped coherently. These spectral projectors arise in deriving the response of the specified source; they are not extra microscopic gates chosen to recognise $|\Omega\rangle$. In the interaction picture,

$$\frac{\mathrm{d}\rho}{\mathrm{d}\tau} = -i[H_{\mathrm{LS}},\rho] + \sum_{j,\varpi>0}\left(L_{j\varpi}\rho L_{j\varpi}^\dagger - \tfrac{1}{2}\{L_{j\varpi}^\dagger L_{j\varpi},\rho\}\right). \tag{36}$$

The same spectrum fixes the Lamb shift, including signed frequencies:

$$\begin{aligned} H_{\mathrm{LS}} &= \sum_{j,\varpi} s(\varpi)A_j^\dagger(\varpi)A_j(\varpi), \\ s(\varpi) &= \frac{1}{3}\,\mathrm{PV}\int_0^\infty \frac{f_\Lambda(\nu)}{\varpi-\nu}\mathrm{d}\nu = \frac{-1-x+x^2e^{-x}\,\mathrm{Ei}(x)}{6\Lambda}, \qquad x = \frac{\varpi}{\Lambda}. \end{aligned} \tag{37}$$

Here $s(0) = -1/(6\Lambda)$ by continuity, and $[H_Q, H_{\mathrm{LS}}] = 0$. The principal-value expression follows by dividing ν^2 by $\varpi - \nu$ and integrating the remaining exponential pole term.

5.4 A convergence criterion, and its verified domain

Dissipation into a dark target is not sufficient for preparation if other dark subspaces remain [9]. Engineered dissipation as a resource for state preparation is established prior art [10]. Here the question is whether the stated bank source supplies the required transitions. For each excited eigenspace define its downward escape operator

$$R_E = \sum_{j,E'<E}\frac{2\pi}{3}f_\Lambda(E-E')P_E Z_{Cj}P_{E'}Z_{Cj}P_E. \tag{38}$$

Positivity must be checked on the complete eigenspace; positive diagonal entries in an arbitrarily chosen degenerate basis would not suffice.

Proposition 5.2 (Conditional preparation in the limit generator)**.** *Suppose H_Q has a unique ground state and every excited R_E is strictly positive on its eigenspace. Then (36) converges to that ground state from every initial density matrix.*

Proof. Using $[H_Q, L_{j\varpi}] = -\varpi L_{j\varpi}$ gives

$$-\frac{\mathrm{d}\langle H_Q\rangle}{\mathrm{d}\tau} = \sum_{j,\varpi>0} \varpi \operatorname{Tr}(L_{j\varpi}^\dagger L_{j\varpi}\rho) \geq 0. \tag{39}$$

Let $\delta_{\min}$ be the smallest distinct positive energy-level spacing, $r_{\min}$ the smallest eigenvalue of any excited R_E, and $W = E_{\max} - E_0$. For $\mathcal{E} = \langle H_Q\rangle - E_0$,

$$-\dot{\mathcal{E}} \geq \delta_{\min} r_{\min} p_{\mathrm{exc}} \geq \frac{\delta_{\min} r_{\min}}{W}\mathcal{E}. \tag{40}$$

Thus $\mathcal{E}$ tends to zero. Since $1 - F_0 = p_{\mathrm{exc}} \leq \mathcal{E}/\Delta_0$, with Δ_0 the ground gap, ground-state fidelity tends to one, and so does convergence in trace distance. □

The minimum level spacing in this proof is not the ground gap. An early numerical bound used the latter in its place; that field is retained as an error in the evidence, and only the corrected bound is used here.

For the six declared cases $J = 1, 2, 8$ and $\Lambda = 8, 16$, all 64 system energy levels are simple and every excited escape rate is positive. The evaluated generators therefore satisfy the criterion. At $J = 2, 8$ their ground state is $|\Omega\rangle$; at $J = 1$ they cool to a different state. The source repairs preparation conditional on the prior selection mechanism; it does not derive the required exchange hierarchy.

For these simple spectra, order populations by energy. The cold population generator is triangular with diagonal $0, -\Gamma_1, \ldots, -\Gamma_{63}$, where Γ_a is the total downward rate. Its spectral gap is $\Gamma_{\min}$. For coherences,

$$\mathcal{D}(|0\rangle\langle a|) = -\tfrac{1}{2}\Gamma_a |0\rangle\langle a|. \tag{41}$$

More generally each gain term lowers the sum of the two state energies, so the dissipator on $|a\rangle\langle b|$ has real triangular diagonal $-(\Gamma_a + \Gamma_b)/2$. The full quantum decay gap is therefore $\Gamma_{\min}/2$, not $\Gamma_{\min}$. The Lamb shift adds imaginary frequencies. At $\Lambda = 8$,

J	Population gap	Full quantum gap
2	1.6940346×10^{-4}	8.4701729×10^{-5}
8	6.9991883×10^{-6}	3.4995941×10^{-6}

These are rates in τ, not physical times at a verified finite coupling. An initial state's population convergence can be faster than the slowest mode; a gap alone is not a complete finite-time error bound. The tested nine-input population times to 99% reach about 3.6×10^5 in slow units. Broader sampled parameter scans do not prove an interval theorem for every $J > J_*$.

5.5 Where energy and quantum information go

The exact microscopic conserved energy is $H_Q + H_B + V_B$. The reduced generator keeps the leading reservoir-limit energy exchange; it is not an exact finite-coupling energy ledger. To see the memory requirement without hiding unsuccessful routes, put $K = \sum_{j,\varpi} L_{j\varpi}^\dagger L_{j\varpi}$ and choose $\mathrm{d}\tau\|K\| \leq 1$. The map

$$W|\psi\rangle = \sqrt{\mathbb{I} - \mathrm{d}\tau K}|\psi\rangle|0\rangle + \sqrt{\mathrm{d}\tau}\sum_{j,\varpi>0} L_{j\varpi}|\psi\rangle|j,\varpi\rangle \tag{42}$$

is exactly isometric because $W^\dagger W = \mathbb{I}$. Assign the output $|j,\varpi\rangle$ energy ϖ and the corresponding type parity. Then

$$(H_Q + H_{\mathrm{out}})W = WH_Q, \qquad (U_Q U_{\mathrm{out}})W = WU_Q. \tag{43}$$

The first identity uses $[H_Q, K] = 0$ and the lowering relation for each jump. The second uses the label export in (33). Including the commuting Lamb-shift unitary leaves these statements intact. Tracing the output recovers the dissipative part of (36) to first order in $\mathrm{d}\tau$.

This dilation exhibits the retained output information. It does not prove that a finite autonomous bank implements an indefinite sequence of fresh outputs. If 64 mutually orthogonal inputs all give the same pure Q state, reversibility requires their orthogonality to move into at least 64 distinguishable bank states. A maximally mixed input exports six bits of entropy; an input entangled with a reference requires preserving six qubits of quantum information. Cooling cannot be credited as a free reset or a clone of an input.

5.6 Spectral regularity and finite-coupling dressing

The cold spectrum cannot be altered solely to accelerate the reduced equation without checking the microscopic energy. Completing the square in (31) gives

$$H_B + V_B = \sum_j \int_0^\infty \nu \left(b_j + \frac{\eta\sqrt{f_\Lambda}}{\sqrt{3}\nu} Z_{Cj} \right)^\dagger \left(b_j + \frac{\eta\sqrt{f_\Lambda}}{\sqrt{3}\nu} Z_{Cj} \right) \mathrm{d}\nu - \frac{\eta^2}{2\Lambda}\mathbb{I}. \tag{44}$$

Thus the total Hamiltonian is bounded below by $H_Q - \eta^2/(2\Lambda)$. The trial state $|\Omega\rangle|\mathrm{vac}\rangle$ has energy E_0 when $|\Omega\rangle$ is the subsystem ground state. If a dressed total ground state exists, these two bounds imply

$$1 - F_\Omega^{\mathrm{dressed}} \le \frac{\eta^2}{2\Lambda\Delta_0}. \tag{45}$$

This controls possible ground-state dressing, not the relaxation time or finite-bank recurrence.

For the broader assumed spectral family

$$f_s(\nu) = \frac{\nu^s e^{-\nu/\Lambda}}{\Gamma(s+1)\Lambda^{s+1}}, \qquad \int \frac{f_s(\nu)}{\nu}\mathrm{d}\nu = \frac{1}{s\Lambda}\ (s>0), \qquad \int \frac{f_s(\nu)}{\nu^2}\mathrm{d}\nu = \frac{1}{s(s-1)\Lambda^2}\ (s>1), \tag{46}$$

the first condition makes the energy lower bound finite; the second makes the static displacement square-integrable. They are different conditions. The choice $s = 2$ satisfies both but is not uniquely derived. At $s = 0$, a definite Z-word and a displaced bank truncated below energy ϵ have variational energy

$$6 - \eta^2 \int_\epsilon^\infty \frac{f_0(\nu)}{\nu}\mathrm{d}\nu = 6 - \frac{\eta^2}{\Lambda} E_1(\epsilon/\Lambda) \longrightarrow -\infty. \tag{47}$$

So that unmodified flat low-energy spectrum is genuinely unbounded below. For $0 < s \le 1$, failure of the second integral alone is not a proof of instability or absence of a ground state.

The preparation result consequently assumes an initially cold continuous reservoir, distinguishable read types, weak coupling, secular resolution and unlimited retained history in the limiting description. None is supplied by the finite clock construction. A finite bank that prepares the clock before appreciable return, with controlled errors and all memory retained, remains unconstructed.

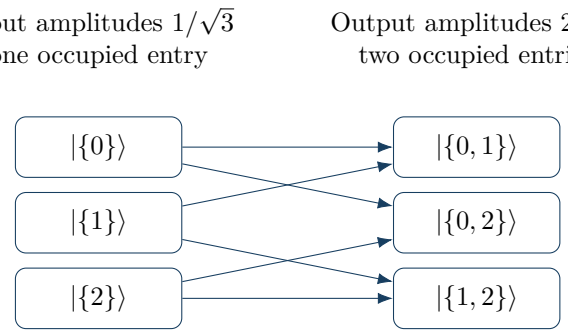


Figure 2: Coherent route counting for three interchangeable storage entries. Every two-entry configuration has two predecessors. The diagram depicts subset transitions; its drawing positions are not physical locations.

6 Coherent storage and its response

6.1 A budget per configuration

Consider d interchangeable two-state storage entries. Their labels carry no spatial location. Let $|A\rangle$ denote a definite occupied subset with $|A| = n$. The adopted push rule is

$$B^\dagger|A\rangle = \frac{1}{\sqrt{d-n}} \sum_{j\notin A} |A \cup \{j\}\rangle \quad (n < d), \qquad B^\dagger|A\rangle = 0 \quad (n = d). \tag{48}$$

Its norm is one on every nonsaturated *basis configuration*. The reverse is its adjoint. This rule assumes coherent any-order access with no which-entry record. It does not assert a state-independent norm bound of one on arbitrary superpositions.

Let $|n\rangle$ be the normalised uniform sum of all $\binom{d}{n}$ subsets. Each target subset of size $n+1$ has $n+1$ predecessors. Thus its amplitude after the push is $(n+1)/\sqrt{(d-n)\binom{d}{n}}$. Using $\binom{d}{n+1} = \binom{d}{n}(d-n)/(n+1)$ gives

$$B^\dagger|n\rangle = \sqrt{n+1}|n+1\rangle, \quad n < d, \qquad B|n\rangle = \sqrt{n}|n-1\rangle. \tag{49}$$

Permutation-invariant operations preserve this symmetric sector if it is initially occupied. The empty bank is such a state. The enhancement $\|B^\dagger|n\rangle\|^2 = n+1$ is coherent addition of indistinguishable routes, not an increased configuration-wise budget.

Writing $J_+ = \sum_j \sigma_j^+$ and $\hat{n}$ for occupation,

$$B^\dagger = J_+(d-\hat{n})^{-1/2}, \qquad [B, B^\dagger] = \mathbb{I} - (d+1)|d\rangle\langle d|, \qquad J_+ = B^\dagger\sqrt{d-\hat{n}}. \tag{50}$$

The inverse is defined as zero at capacity. This is the truncated Holstein–Primakoff boson on the collective Dicke sector, whose underlying algebra is established [11–13]. The derivation identifies what the adopted normalisation implements; it does not derive Bose statistics or the spin–statistics relation.

A constant-amplitude ladder instead has $B^\dagger|n\rangle = |n+1\rangle$ in its interior. Last-in, first-out ordering does not require constant amplitudes: a stack could be given the square-root law as an additional input. Hence the result does not prove that any-order access is necessary. Its merit here is that the chosen matrix elements follow from the stated configuration rule and route counting.

6.2 An exactly soluble single-record comparison

To separate a ladder effect from the more complex transaction energy, first take a distinct calibration action,

$$H_{\mathrm{ex}} = \varepsilon_R n_R + \varepsilon_B \hat{n} + g(l_R B^\dagger + l_R^\dagger B), \qquad B^\dagger|n\rangle = f_{n+1}|n+1\rangle. \tag{51}$$

This is not yet the gated module (3). It conserves $n_R + \hat{n}$. In the block $\{|1,n\rangle, |0,n+1\rangle\}$,

$$H_n = \begin{pmatrix} \varepsilon_R + n\varepsilon_B & g f_{n+1} \\ g f_{n+1} & (n+1)\varepsilon_B \end{pmatrix}. \tag{52}$$

Its eigenvalues are the mean diagonal energy plus or minus $\sqrt{\Delta^2/4 + g^2 f_{n+1}^2}$, where $\Delta = \varepsilon_R - \varepsilon_B \neq 0$. Follow the branches continuously from $g = 0$. If R_n is the adjacent bank-level gap on the filled-record branch minus that on the empty-record branch, cancellation of the intermediate square root yields exactly

$$R_n = \operatorname{sgn}\Delta \left[\sqrt{\Delta^2/4 + g^2 f_{n+2}^2} - \sqrt{\Delta^2/4 + g^2 f_n^2}\right], \tag{53}$$

$$R_n = \frac{g^2}{\Delta}(f_{n+2}^2 - f_n^2) + O(g^4). \tag{54}$$

For the square-root ladder, the second-order interior response is $2g^2/\Delta$. The exact response depends on n at finite g, and the capacity boundary changes the formula through $f_{d+1} = 0$. A flat interior ladder gives zero response when both endpoints are interior. A capacity edge must not be mistaken for a uniform clock effect.

Equation (53) also fixes the sign for this calibration model: for $g \neq 0$ and the square-root interior ladder, the filled record reduces the gap exactly when $\varepsilon_B > \varepsilon_R$. The storage law does not fix that energy ordering. These dressed spectral gaps require a specified readout before they become an operational clock comparison; the next construction supplies one.

7 Response to the full transaction energy

7.1 The action and the controlled reduction

Attach the finite occupation bank (49) to the full source (3):

$$H = H_S \otimes \mathbb{I} + \mathbb{I} \otimes \omega\hat{n} + g(L_\lambda \otimes B^\dagger + L_\lambda^\dagger \otimes B). \tag{55}$$

The gate appears in both the source energy and the coupling. This is a specified shared-bank extension, not an identification with the counterpart clock C. The spectrum, coupling and coherent probe preparation are inputs. All $8(d+1)$ states and both directions of transfer are retained.

Take ω greater than the source bandwidth and g sufficiently small that adjacent bank-number bands remain isolated. The explicit form of A_S in (3) gives $\|A_S\| \leq 2 + |\lambda|$ by the triangle inequality, since each X_j and $n_0 n_1 X_2$ has norm one. Thus, for the tested $0 \leq \lambda \leq 1$, the bandwidth is at most $2(2+\lambda) \leq 6$, below both tested bank spacings $\omega = 8, 16$. In an H_S energy

basis, second-order block elimination gives

$$H_{\mathrm{eff},n} = H_S + n\omega\mathbb{I} + g^2 Q_n + O(g^4),$$
$$Q_n = f_{n+1}^2 B_+ + f_n^2 B_-, \tag{56}$$
$$(B_+)_{ij} = \frac{1}{2}\sum_k L_{ki}^* L_{kj}\left(\frac{1}{E_i - E_k - \omega} + \frac{1}{E_j - E_k - \omega}\right), \tag{57}$$
$$(B_-)_{ij} = \frac{1}{2}\sum_k L_{ik} L_{jk}^*\left(\frac{1}{E_i - E_k + \omega} + \frac{1}{E_j - E_k + \omega}\right). \tag{58}$$

Here $L = L_\lambda$. To obtain these expressions, write $H = H_0 + gV_1$ and choose an anti-Hermitian off-band generator with $S_{ab} = (V_1)_{ab}/(E_a^0 - E_b^0)$. Then $[S, H_0] = -V_1$ off the bands and $e^{gS}He^{-gS}$ contributes $g^2[S, V_1]/2$ within a band. Its two denominators give the Hermitian averages in (57)–(58). One intermediate upward or downward bank step contributes f_{n+1}^2 or f_n^2. An odd number of elementary transfers cannot return to the same bank occupation, explaining the absence of an isolated-band third-order term. This is standard effective-Hamiltonian perturbation theory [14], with a specified choice of subspace and a gap assumption.

For adjacent interior steps of the square-root ladder,

$$K = Q_{n+1} - Q_n = B_+ + B_-. \tag{59}$$

At the terminal step $n = d - 1$, it is instead $-dB_+ + B_-$. In the interior $\operatorname{Tr} K = 0$: exchange i and k in the trace of (58), and its terms cancel those of (57). Consequently a universal affine response would have to be proportional to $H_S - 3\mathbb{I}$. The reference three is the mean energy of this module, not a derived absolute vacuum energy.

7.2 A readout of the reduced response

Let X_n embed the bare source at occupation n, and let Π_n be the exact projector onto the isolated interacting band continued from it. The positive-overlap isometry

$$W_n = \Pi_n X_n (X_n^\dagger \Pi_n X_n)^{-1/2} \tag{60}$$

fixes the identification of source vectors with dressed states. It is defined when the overlap matrix is invertible. Use the exact reduced matrices $H_{\mathrm{eff},n} = W_n^\dagger H W_n$ and the observable $C_n = W_n W_{n+1}^\dagger$. For the declared input $(W_n|v\rangle + W_{n+1}|v\rangle)/\sqrt{2}$,

$$z_n(u) = 2\langle C_n\rangle_u = \langle v|e^{iH_{\mathrm{eff},n}u}e^{-iH_{\mathrm{eff},n+1}u}|v\rangle, \qquad -\operatorname{Im}\dot{z}_n(0) = \omega + g^2\langle v|K|v\rangle + O(g^4). \tag{61}$$

The real and imaginary quadratures of C_n are ordinary Hermitian observables. This connects the reduced coefficients to a full-system coherence experiment. It assumes the preparation and measurement of dressed states; it does not derive an autonomous detector. Nor does an initial derivative prove a constant rate at later times if the two reduced source Hamiltonians do not commute.

In the registered tests, the exact reduced and full-Hamiltonian coherences agree to 1.53×10^{-13} over the declared probes. Substitution of bare, undressed coherences fails the control. Capacity $d = 6$ was compared with $d = 8$ on two interior responses; the exact matrices changed by at most 1.99×10^{-9}. These are finite convergence checks, not an unlimited-capacity theorem.

7.3 The positive free-record identity

The stationary response is the complete energy-block-diagonal part

$$K_{\mathrm{st}} = \sum_E P_E K P_E. \tag{62}$$

Full degeneracies remain inside each P_E. Even a universal K_{st} is weaker than a universal full operator or a common finite-time clock rate.

Proposition 7.1 (Free records at second order)**.** *For m independent records with $H_S = m\mathbb{I} + A$, $A = \sum_{j=1}^{m} X_j$ and $L = \sum_j l_j$, the formal stationary same-occupation coefficient is*

$$K_{\mathrm{st}} = \frac{A}{4 - \omega^2}, \qquad \omega \neq 0, 2. \tag{63}$$

It is an operational dispersive response when the required bank bands are isolated; $\omega > 2m$ and sufficiently small g are a sufficient regime.

Proof. Decompose $L = \sum_\nu L_\nu$ into Bohr components, $[H_S, L_\nu] = \nu L_\nu$. There are only $\nu = 0, \pm 2$. In the X eigenbasis for one record,

$$l = \frac{1}{2}\begin{pmatrix} 1 & -1 \\ 1 & -1 \end{pmatrix}, \quad L_0 = X/2, \quad L_{+2} = -|+\rangle\langle -|/2, \quad L_{-2} = |-\rangle\langle +|/2. \tag{64}$$

Terms on different records commute, so

$$[L_0, L_0^\dagger] = 0, \qquad [L_{+2}, L_{+2}^\dagger] = A/4, \qquad [L_{-2}, L_{-2}^\dagger] = -A/4. \tag{65}$$

Stationary projection of (57)–(58) retains pairs of equal Bohr frequency and gives

$$K_{\mathrm{st}} = \sum_\nu \frac{[L_\nu, L_\nu^\dagger]}{\omega + \nu} = \frac{A}{4}\left(\frac{1}{\omega + 2} - \frac{1}{\omega - 2}\right) = \frac{A}{4 - \omega^2}. \tag{66}$$

The argument is an operator identity inside the complete energy blocks, not a fit to selected eigenvalues. □

Thus the stationary response is exactly energy-proportional *at second order*, for any finite number of independent records. For positive ω the coefficient is negative precisely when $\omega > 2$, the single-record transition energy in these units. Higher source energy then reduces the probe frequency at this order. Neither packet conservation nor configuration-wise normalisation fixes this ordering. At finite g higher-order corrections remain.

One-step denominators alone do not establish an isolated clock. At $\omega = 1$ a two-packet resonance mixes occupations already at order g^2, even though the denominators at $\omega = 2$ are avoided. At $\omega = 4$, two free records have a third-order resonant path, with a competing second-order diagonal splitting. Appendix B gives both blocks. A divergent perturbative expression at resonance is a failure of the reduction, not a divergence of the finite Hermitian Hamiltonian or proof that no clock can exist.

7.4 The interacting module fails the energy-only test

For a source eigenstate $|i\rangle$, the response is

$$k_i = \sum_k \left[\frac{|L_{ki}|^2}{E_i - E_k - \omega} + \frac{|L_{ik}|^2}{E_i - E_k + \omega}\right]. \tag{67}$$

This depends on all available transition energies and matrix elements. A universal stationary response would require the same coefficient multiplying $E_i - 3$ for every state, together with the corresponding identity in degenerate blocks.

For $\lambda = 1$ and $\omega = 8$, Table 3 shows three energy-paired comparisons. The members of each pair have identical packet-count distributions, because word parity maps one eigenstate to

Source energies (E_-, E_+)	Coefficients (k_-, k_+)	$(k_+ - k_-)/(E_+ - E_-)$
$(0.657077, 5.342923)$	$(+0.0440617, -0.0440617)$	-0.0188063
$(1.186393, 4.813607)$	$(+0.0447114, -0.0447114)$	-0.0246533
$(2.529317, 3.470683)$	$(+0.0211260, -0.0211260)$	-0.0448836

Table 3: Stationary second-order coefficients for the gated module, with $\omega = 8$. Actual leading frequency corrections are $g^2 k_i$. The free-record slope would be $1/(4 - 8^2) = -1/60$.

its opposite-energy partner without changing word probabilities. Nevertheless the response-to-energy slopes differ by a factor of approximately 2.39. A single coefficient cannot describe them.

The mechanism can be made explicit. For (3), $[N_S, H_S] = L^\dagger - L$. In a real energy eigenbasis, $L + L^\dagger = H_S - 3\mathbb{I}$ gives $L_{ik} = -L_{ki}$ off the diagonal, and the commutator gives $L_{ik} = (E_i - E_k)(N_S)_{ik}/2$. Substitution in (67) yields

$$k_i = \sum_k \frac{(E_i - E_k)^3 |(N_S)_{ik}|^2}{2[(E_i - E_k)^2 - \omega^2]}. \tag{68}$$

The diagonal $k = i$ contribution cancels. Equation (68) identifies the missing requirement: a transition-strength sum rule would have to reduce this expression to one common multiple of total energy, including the gated interaction. The tested law supplies no such identity.

A larger bank quantum does not repair the leading relative discrepancy. Put $A = H_S - 3\mathbb{I}$ and $C = [L, L^\dagger]$. Expanding the denominators gives

$$K = \frac{C}{\omega} + \frac{D}{\omega^2} + O(\omega^{-3}), \qquad 2D = [L - L^\dagger, C]. \tag{69}$$

The coefficient before this simplification is

$$D = -\tfrac{1}{2}([H_S, L^\dagger]L + L^\dagger[L, H_S] + [H_S, L]L^\dagger + L[L^\dagger, H_S]). \tag{70}$$

For $H_S = 3\mathbb{I} + L + L^\dagger$, substituting the commutators $[H_S, L^\dagger] = C$ and $[H_S, L] = -C$ gives the second identity in (69).

Since $L = (A - [N_S, A])/2$, $C = \frac{1}{2}[A, [N_S, A]]$ has zero block-diagonal part in the A eigenspaces. If D_{st} were proportional to A, every ratio

$$\frac{\mathrm{Tr}(A^{2r-1} 2D)}{\mathrm{Tr}(A^{2r})} \tag{71}$$

would be the same. Exact finite-matrix arithmetic for the gated module gives

$$-\frac{22}{9}, \qquad -\frac{94}{41}, \qquad -\frac{446}{201} \quad (r = 1, 2, 3), \tag{72}$$

The corresponding integer numerator/denominator pairs are $(-44, 18)$, $(-188, 82)$ and $(-892, 402)$, obtained directly from the eight-state transaction matrices. The free comparison gives -2 in all three cases. Their inequality rules out proportionality of the leading stationary coefficient. This analytic explanation was obtained after the initial numerical result and is recorded as such. Raising ω reduces the absolute effect without removing this leading relative obstruction.

The tested alternatives with other interaction gates also fail the stationary energy-only diagnostic. The scope is those specified actions and readouts. The calculation is not a theorem that all interactions or all possible dressed observables must fail.

8 Testing the counterpart clock itself

The occupation probe above is an added construction. It is therefore important to test the unchanged counterpart clock (20), rather than assuming the two probes are interchangeable.

8.1 The selected-state reading has no extra rate

Equation (25) is independent of J, while the full state's eigenvalue changes from 6 to $6 - 3J$. For that state and that reading, exchange changes the global energy but does not generate an additional energy-dependent conditional rate. This exact zero is specific to the stated conditional observable. It does not exclude every alternative dressed clock.

8.2 A loaded clock can detect equal-energy coherence

A second experiment prepares a source eigenstate $|v\rangle$ and a clock coherence $(|a\rangle + |b\rangle)/\sqrt{2}$ between distinct clock energies. This disturbs the selected state and is a different preparation. At $u = 0$, partial tracing the full commutator gives the exact clock generator $H_C + JT_v$, with

$$T_v = \mathrm{Tr}_S[V(\mathbb{I} \otimes |v\rangle\langle v|)]. \tag{73}$$

For $z_{ab}(u) = 2\langle a|\rho_C(u)|b\rangle$,

$$-\operatorname{Im} \dot{z}_{ab}(0) = E_a^C - E_b^C + J[(T_v)_{aa} - (T_v)_{bb}]. \tag{74}$$

This is an exact initial derivative at every J, not a late-time constant-rate assertion.

There is a particularly simple counterexample. Let integer word labels use bit 0 as the least significant bit, and set

$$D_0 = \frac{|1\rangle - |2\rangle}{\sqrt{2}}, \qquad D_1 = \frac{|5\rangle - |6\rangle}{\sqrt{2}}, \qquad D_\pm = \frac{D_0 \pm D_1}{\sqrt{2}}. \tag{75}$$

The root transactions cancel on D_0, D_1, and their gated prerequisites are never both occupied. Hence $H_S D_\pm = 3D_\pm$ for every λ. Both states have probability $1/2$ in word-count one and $1/2$ in word-count two. Yet they have opposite eigenvalues of X_2, so

$$\langle l_0\rangle = \langle l_1\rangle = 0, \quad \langle l_2\rangle_{D_\pm} = \pm\tfrac{1}{2}, \qquad T_{D_\pm} = \pm X_{C2}/2. \tag{76}$$

Since $[X_{C2}, H_C] = 0$, choose distinct-energy clock states in opposite X_{C2} sectors. Their initial frequency shifts in (74) reverse sign between D_+ and D_-. Thus the interaction detects information within a fixed-energy sector. Equal energy and equal packet-count statistics are insufficient to determine its response.

This witness concerns the native matching exchange, whose third-label transfer is ungated. The occupation probe in (55) instead couples through the gated L_λ. The difference is physical and stated, not a change of notation. Even three free records fail the energy-only test for the native loaded readout: a source with X signs $(+, +, -)$ gives $T_v = (X_{C0} + X_{C1} - X_{C2})/2$, so equal clock gaps associated with labels 0 and 2 have opposite fractional shifts. This does not contradict (63), which concerns a different bank action, reduction and observable.

An explicitly supplied energy-product interaction can pass the desired diagnostic. That is a useful positive control for the measurement, but inserting it would assume the property under investigation. No such replacement is made in either negative result.

9 Relation to prior work and the remaining problem

9.1 What the construction inherits

Relational time in a stationary quantum state is the Page–Wootters proposal [1]. The conditioning and measurement-accounting framework used here belongs to its subsequent development [2]. Results about factorisation, clock ambiguity and equivalence between relational descriptions have stated assumptions about clocks, constraints and subsystem structure [3, 15]. Our counterpart rule specifies a factorisation and an action; it does not prove uniqueness of that choice.

Finite clocks introduce spectral compatibility, measurement resolution and periodicity issues [4–6]. Section 3 supplies an example in which improving a fixed-window approximation does not give exact stationarity or full-period convergence. A clock-dependent conditional state, an external diagnostic-time frequency, and a physical observer's reading remain distinct objects.

The state (21) is maximally entangled under a local mirror transformation. At inverse temperature $\beta = 0$, the thermofield double

$$|\mathrm{TFD}_\beta\rangle = Z^{-1/2} \sum_a e^{-\beta E_a/2} |E_a\rangle_L |E_a^*\rangle_R \tag{77}$$

reduces to such a maximally entangled vector. Entangled parent-Hamiltonian design and the distinction between selecting a ground state and cooling into it are prior art [7]. Our example gives the two modules complementary energies through a vacancy rule and retains a simple matching exchange. It does not make general parent-Hamiltonian engineering new.

The storage amplitudes implement the known Dicke and Holstein–Primakoff algebra [11–13]. Their interpretation as a configuration-normalised bank rule exposes the resource premise; it does not derive bosonic statistics from nonquantum assumptions. The cold limit uses established dissipative preparation methods [8–10], and its finite-bank extension remains open.

9.2 Comparison with assumed gravitational clock couplings

Interactions between a clock and a system generally change conditional evolution; they need not reduce to a scalar rate change. Smith and Ahmadi derive a general interacting-clock conditional kernel [16]. Their gravitational example starts from an energy-product coupling with a supplied distance and gravitational constant. Castro Ruiz, Giacomini and Brukner analyse the implications of

$$H_A + H_B - \frac{G}{c^4 x} H_A H_B, \tag{78}$$

with separation x supplied [17]. These works study consequences of a gravitational interaction; they do not claim that arbitrary record transfers generate it.

A close comparison is Singh and Friedrich [18]. Their constraint includes the explicit product

$$\mathcal{J} = p_t + H_S + \frac{p_t H_S}{\Lambda} \approx 0, \qquad H_{\mathrm{eff}} = H_S(\mathbb{I} + H_S/\Lambda)^{-1}. \tag{79}$$

For commuting subsystem energies $H_S = H_A + H_B$, expansion gives

$$H_{\mathrm{eff}} = H_A + H_B - \frac{H_A^2 + H_B^2 + 2H_A H_B}{\Lambda} + O(\Lambda^{-2}). \tag{80}$$

The cross term follows from the chosen constraint. Matching its coefficient to gravity uses their identification $1/\Lambda = G/(2r)$, with r a constant classical separation. This is a conditional construction, but supplies the energy-product coupling that our transactions are being asked to produce.

Cafasso and collaborators specify pairwise clock-energy products and coupling constants before deriving interaction transfer [19]. The clock calculations in chapter 7 of Favalli's treatment use specified gravitational potentials or their relativistic counterparts [20]. These inputs are appropriate to those questions. They do not derive distance, universal coupling or its coefficient from the record transactions studied here.

The difference is precise. An assumed $H_A H_B$ interaction is energy-only by construction. Equation (67) instead sums matrix elements of transaction operators. The free-record identity shows that this sum can collapse to total energy. The counterexamples show why that collapse cannot simply be assumed to survive interactions or a change of observable.

9.3 Why a negative frequency shift is not yet gravity

No distance or operational spatial relation has been derived, so there is no inverse-distance potential, field propagation law, tidal observable or gravitational constant to compare with experiment. The energy-centred coefficient also does not assign an absolute gravitational role to an arbitrary additive constant in a finite Hamiltonian.

Quantum formulations of the equivalence principle distinguish rest, inertial and gravitational energy operators. Agreement of selected diagonal expectations is weaker than equality of those operators [21]. The free stationary identity is therefore a limited positive result, not the equivalence principle. Established scattering arguments for universal gravitational coupling use relativistic and massless-spin-two assumptions absent here [22]; importing their conclusion would not derive those assumptions from records.

The three binary labels are not three physical generations. They define a finite test module. Its gated interaction has not produced a proton, a field-theoretic scattering amplitude or a measured mass ratio. Such claims require additional derivations and an observable map. No empirical particle data enters any coefficient reported here.

9.4 A focused requirement for further progress

For preparation, the bank must receive every obstructing conserved label as well as energy, and its low-entropy acceptance resource and retained memory must be explained. For a universal stationary clock response, a transaction law must imply a relation of the form

$$\sum_E P_E(B_+ + B_-)P_E = a\left(H_S - \frac{\operatorname{Tr} H_S}{\dim \mathcal{H}_S}\mathbb{I}\right), \tag{81}$$

with one coefficient for the full interacting source, followed by an operational readout and a controlled approximation. Equation (68) identifies the missing transition-strength identity; (76) tests whether fixed-energy coherence is incorrectly visible to an energy-only probe.

Increasing the capacity of an unchanged source or fitting a coefficient to each eigenstate does not meet these requirements. A successor must state an interaction or symmetry and show why it enforces the identity. A finite preparation model with complete energy and memory accounting would also be useful even without universal energy response. The construction remains a rigorous pedagogical example in that case.

10 Conclusions

A vacancy counterpart of a finite record rule generates complementary energies, and matching exchange selects a state supporting exact conditional evolution. This reduces the independently specified clock data, while leaving the counterpart rule and exchange hierarchy as assumptions.

Closed evolution does not prepare the selected eigenstate. A finite receiving bank exposes a symmetry obstruction; a source that exports the label permits conditional preparation in a cold continuous-reservoir limit.

Configuration-wise normalisation gives a truncated bosonic ladder. Its dispersive coupling to independent records has a stationary second-order response proportional to energy, with a sign determined by the energy ordering. The tested gated records violate that proportionality, including in the leading large-frequency coefficient. The native counterpart clock gives an exact equal-energy counterexample under a different readout.

The work establishes explicit models, derivations and reproducible limitations, not a physical vacuum substrate or emergent spacetime. Compatible energies, selected correlations, preparation, access and universal energy response are separate demands on a transaction rule. The missing implication can now be stated and tested mathematically.

Computational practice and availability

All numerical results come from retained finite-model packages and separately implemented reviews. The evidence was consolidated in M5 after clean exports of committed source trees were replayed. Baselines, deliberate faults, original failures and corrections are mapped in Appendix C. A successful implementation check is not empirical validation; two implementations of one model are not two physical observations.

The supporting code, numerical data, registrations, corrections and implementation reviews are archived on Zenodo [23]. The cited concept DOI identifies the evolving collection; the exact evidence release used here is version 1.0.0, doi:10.5281/zenodo.24109717. It includes portable replay commands and a distribution manifest. Scientific sources and saved results are unchanged from the frozen evidence commit. Third-party article texts, private coordination logs and the administrative database are excluded. The paper's separate Zenodo record contains this PDF and editable LaTeX source, including build instructions and the evidence map.

Acknowledgements and disclosure

The research and manuscript were developed with assistance from Codex and Claude for algebra, programming, cross-checking, literature retrieval and drafting. Their separately constructed implementations and critiques are recorded. This process is computational verification, not independent experimental confirmation or journal peer review. David Elliman is the author; the author approved this preprint and its archival release.

A Spectrum of the three-record module

The explicit form in (3) shows that $[X_2, A_S] = 0$ for every λ. For the spectrum quoted here set $\lambda = 1$ and work in the X_2 eigenvalue sector $s = \pm 1$. On the other two bits, $A_s = X_0 + X_1 + s n_0 n_1$. The antisymmetric vector $(|01\rangle - |10\rangle)/\sqrt{2}$ has eigenvalue zero. In the remaining symmetric basis $\{|00\rangle, (|01\rangle + |10\rangle)/\sqrt{2}, |11\rangle\}$,

$$A_s = \begin{pmatrix} 0 & \sqrt{2} & 0 \\ \sqrt{2} & 0 & \sqrt{2} \\ 0 & \sqrt{2} & s \end{pmatrix}, \qquad \det(x\mathbb{I} - A_s) = x^3 - sx^2 - 4x + 2s. \tag{82}$$

Multiplying the two cubic factors and restoring the two zero modes gives

$$\det(x\mathbb{I} - A_S) = x^2(x^6 - 9x^4 + 20x^2 - 4). \tag{83}$$

The nonzero roots are irrational: the rational-root theorem restricts rational roots of the monic sixth-degree factor to $\pm1, \pm2, \pm4$, and substitution excludes them. Opposite pairs give (4) after adding three.

For $B = 8$, $E_* = 7$ and even integer d_C, exact matching to the uniform clock requires $x = 4 - 8n/d_C$, a rational number. Only $x = 0$ can occur. The exact shell therefore contains only the two dark source modes at energy three and a single clock level $n = d_C/2$. It cannot represent nontrivial source dynamics. This is a limitation of this rational uniform-clock family, not of every finite relational clock.

B Resonances and the order of the response

The same-occupation coefficient in (63) cannot discard other states degenerate with its chosen band. The examples here use finite occupation states and the same free-record action, without spatial interpretation.

B.1 A second-order two-packet resonance

For one free record, $H_S = \mathbb{I} + X$, the energies of $|+\rangle$ and $|-\rangle$ are two and zero. At $\omega = 1$, $|+, n\rangle$ and $|-, n+2\rangle$ have equal unperturbed energy. The first direct matrix element vanishes, but two transactions connect them. For $n = 0$ the full second-order block is

$$H_{\text{block}} = 2\mathbb{I} + g^2 \begin{pmatrix} 0 & -1/\sqrt{2} \\ -1/\sqrt{2} & -1 \end{pmatrix} + O(g^4), \tag{84}$$

in the ordered basis $\{|+, 0\rangle, |-, 2\rangle\}$. Summing the two intermediate source states at bank occupation one, with the l matrix in the proof of (63), gives the off-diagonal entry. At general n its magnitude is $\sqrt{(n+1)(n+2)}/2$.

Diagonal splitting and mixing in (84) have the same order. The largest limiting bare-state weight is

$$\frac{1 + 1/\sqrt{3}}{2} = 0.788675\ldots, \tag{85}$$

which does not approach one as $g \to 0$. Avoiding the one-step pole was insufficient to identify an independent occupation clock.

At first and second order, positive cross-occupation free-record resonances occur at $\omega = 2$ or 1: one or two transactions change source energy in multiples of two while changing occupation by one or two. Zero frequency is singular; same-occupation source degeneracies also remain. This is not an all-orders exclusion of other resonances.

B.2 A third-order path at $\omega = 4$

For two free records, $a = |{+}{+}, n\rangle$ and $b = |{-}{-}, n+1\rangle$ have common energy $E_0 = 4 + 4n$ at $\omega = 4$. Retaining the pair gives

$$H_{\text{block}} = E_0\mathbb{I} + g^2 \begin{pmatrix} -n/6 - 1/2 & 0 \\ 0 & n/6 - 1/6 \end{pmatrix} - \frac{g^3\sqrt{n+1}}{6} \begin{pmatrix} 0 & 1 \\ 1 & 0 \end{pmatrix} + O(g^4). \tag{86}$$

The third-order element is the path sum

$$\sum_{r,s \notin \{a,b\}} \frac{\langle b|V_1|s\rangle\langle s|V_1|r\rangle\langle r|V_1|a\rangle}{(E_0 - E_s)(E_0 - E_r)}. \tag{87}$$

In an unnormalised occupation basis where raising has amplitude one and lowering amplitude n, grouping by successive bank changes gives

Bank changes	Path sum
$(+1,+1,-1)$	$-(n+2)/12$
$(+1,-1,+1)$	0
$(-1,+1,+1)$	$n/12$

Their sum is $-1/6$; normalising occupation states multiplies it by $\sqrt{n+1}$. Thus the coefficient is derived without fitting a level splitting.

The second-order separation is $g^2(n+1)/3$, so mixing at fixed $\omega = 4$ is only $O(g)$ and vanishes in the limit, unlike (84). The leading avoided-crossing centre and gap are

$$\omega_* = 4 - \frac{n+1}{3}g^2 + O(g^4), \qquad \Delta_{\text{avoided}} = \frac{g^3\sqrt{n+1}}{3} + O(g^4). \tag{88}$$

Exact finite matrices were checked at capacity eight, $n = 0, 1, 2, 3$ and $g = 0.08, 0.04, 0.02, 0.01$. A separate review confirmed the diagonal coefficients and shifted crossing. A higher-order path is retained without turning it into an order-one obstruction at a lower perturbative order.

C Reproducibility, corrections and claim provenance

C.1 What was replayed

Scientific implementations use Python, NumPy and SciPy, with no imports from previous spatial-lattice code. The original environment was Python 3.13.7, NumPy 2.4.4 and SciPy 1.17.1, with single-threaded BLAS. Complete finite spaces, reverse routes and named memory factors are retained. Reductions, limits and supplied measurements are identified explicitly.

The constructor evidence tree is `84122c9`; the review tree was replayed at `97dfae2`. The constructor replay record is committed at `df0ddca`. Clean `git archive` exports isolate calculations from uncommitted files. A pristine copy is retained separately from the execution copy, including for scripts that use fixed output names.

Constructor-side consolidation reproduces 32 main processes: ten baselines with exit zero and 22 faults with exit one. Eight additional processes reproduce post-hoc checks and their faults; original M3's accuracy failure also replays with exit one. Scientific JSON values agree at absolute/relative tolerance 10^{-9}, numeric arrays at the same tolerance, and text arrays exactly. Runtime, timestamps and resource-use fields are excluded explicitly. All 980 pristine files match their committed Git blobs afterwards. A separate reviewer replay of three constructor baselines and five cross-package comparisons agrees. These establish reproducibility on the stated environment, not statistical significance or physical truth.

Three mistakes in the replay harness were retained and corrected: treating text-array labels as numbers, omitting a runtime-field spelling and using a CLI fault name instead of its saved directory alias. A review-side comparison initially differed only in its exit-footer format. No scientific source or tolerance changed. The supporting archive retains these logs.

C.2 Evidence units and corrections

Quoted error bounds are rounded upward at their stated precision; central estimates are rounded to the nearest stated digit.

Unit identifiers in Table 4 are reproducibility labels. The companion `EVIDENCE.md` gives full directories, result paths and commands.

Table 4: Claim-to-evidence map. Each unit has a separate implementation review.

Unit	Claim used here	Scope or correction retained
PW1	Finite-clock bound and benchmark; stationary matched spectrum	Fixed-window convergence only. Instrument error 0.0006241 is an upper bound.
PW2	Counterpart identity; selected eigenstate and threshold; $J = 2$ gap from M3b	Matched strengths and hierarchy assumed; readout efficiency is family dependent.
PW3	Finite-bank failure and sector obstruction	Nine word inputs; four sector-admissible review inputs also fail in the sampled window. Symmetry proof is post hoc.
PW4	Cold response, label export, escape criterion, memory	Reservoir limit; level-spacing bound corrected; full decay gap is half the population gap.
M2	Storage rule, finite ladder and two-state blocks	Budget per configuration; interior uniformity at second order; LIFO not ruled out.
M3	Dispersive response, dressed readout and interacting mismatch	Original six accuracy failures retained; refinement at unchanged tolerance. Moment obstruction is post hoc.
M3b	Native conditional zero and equal-energy witness	Two readouts; initial derivative is not a persistent late-time rate.
M4	Free-record sign and resonant corrections	Original two accuracy failures retained. Extrapolation tests a limiting coefficient. Third-order follow-up separately checked.
M0	Literature and exact prior-art identifications	21 metadata checks; eight priority comparisons independently checked at equation level.

M3's original $g = 0.02$ checks missed a 0.1% spectral bar in six cases. The recorded amendment added $g = 0.01$, retaining the action, original samples and tolerance; the finest error is at most 0.03746%. M4's original Richardson pair $g = 0.04, 0.02$ missed its 10^{-4} coefficient-accuracy bar twice at $\omega = 0.6$. The declared replacement pair $0.01, 0.005$ passes the same bar, with worst relative error 7.69×10^{-7}. Extrapolation estimates a $g \to 0$ coefficient, not an exact finite-g equality. The failed outputs are preserved.

PW4's baseline field `energy_decay_bound` used the ground gap instead of the minimum level spacing. It is not used here as a valid bound. The corrected coefficient, population/coherence distinction and low-energy spectral qualification are explicit. A sampled search for dark states or crossings is not a proof for every real coupling.

C.3 Reference verification

The bibliography contains 22 published works whose DOI metadata were checked against publisher/Crossref records and available primary manuscripts. Detailed comparisons with Smith–Ahmadi, Singh–Friedrich, Cafasso and collaborators, Castro Ruiz and collaborators, Cottrell and collaborators, Emary–Brandes, Favalli's chapter 7 and Chataignier and collaborators

were also checked separately at equation level. The selected-state and finite-ladder identifications were instantiated algebraically.

Full text of the original Page–Wootters and Holstein–Primakoff articles was unavailable in the recorded retrieval; Davies and Weinberg were used at contextual abstract/metadata scope. Their detailed mathematical roles here are either derived explicitly or supported by accessible primary sources cited alongside them. Favalli's book was read selectively, not in full. These limits are recorded, and no priority claim is inferred from the search. The additional Verstraete–Wolf–Cirac citation was checked against publisher-deposited metadata and the authors' manuscript for its dissipative-preparation claim; its lattice constructions are not imported into this model.

The supporting-software entry was verified against its published Zenodo record; it identifies the exact version used and the concept DOI for the collection.

References

[1] Don N. Page and William K. Wootters. Evolution without evolution: Dynamics described by stationary observables. *Physical Review D*, 27:2885–2892, 1983. doi: 10.1103/PhysRevD.27.2885.

[2] Vittorio Giovannetti, Seth Lloyd, and Lorenzo Maccone. Quantum time. *Physical Review D*, 92:045033, 2015. doi: 10.1103/PhysRevD.92.045033.

[3] Philipp A. Höhn, Alexander R. H. Smith, and Maximilian P. E. Lock. Trinity of relational quantum dynamics. *Physical Review D*, 104:066001, 2021. doi: 10.1103/PhysRevD.104.066001.

[4] Tommaso Favalli and Augusto Smerzi. Time Observables in a Timeless Universe. *Quantum*, 4:354, 2020. doi: 10.22331/q-2020-10-29-354.

[5] Mischa P. Woods, Ralph Silva, and Jonathan Oppenheim. Autonomous Quantum Machines and Finite-Sized Clocks. *Annales Henri Poincaré*, 20:125–218, 2019. doi: 10.1007/s00023-018-0736-9.

[6] Leonardo Chataignier, Philipp A Höhn, Maximilian P E Lock, and Fabio M Mele. Relational dynamics with periodic clocks. *New Journal of Physics*, 28:034504, 2026. doi: 10.1088/1367-2630/ae46d0.

[7] William Cottrell, Ben Freivogel, Diego M. Hofman, and Sagar F. Lokhande. How to build the thermofield double state. *Journal of High Energy Physics*, 02:058, 2019. doi: 10.1007/JHEP02(2019)058.

[8] E. B. Davies. Markovian master equations. *Communications in Mathematical Physics*, 39:91–110, 1974. doi: 10.1007/BF01608389.

[9] B. Kraus, H. P. Büchler, S. Diehl, A. Kantian, A. Micheli, and P. Zoller. Preparation of entangled states by quantum Markov processes. *Physical Review A*, 78:042307, 2008. doi: 10.1103/PhysRevA.78.042307.

[10] Frank Verstraete, Michael M. Wolf, and J. Ignacio Cirac. Quantum computation and quantum-state engineering driven by dissipation. *Nature Physics*, 5(9):633–636, 2009. doi: 10.1038/nphys1342.

[11] R. H. Dicke. Coherence in Spontaneous Radiation Processes. *Physical Review*, 93:99–110, 1954. doi: 10.1103/PhysRev.93.99.

[12] T. Holstein and H. Primakoff. Field Dependence of the Intrinsic Domain Magnetization of a Ferromagnet. *Physical Review*, 58:1098–1113, 1940. doi: 10.1103/PhysRev.58.1098.

[13] Clive Emary and Tobias Brandes. Chaos and the quantum phase transition in the Dicke model. *Physical Review E*, 67:066203, 2003. doi: 10.1103/PhysRevE.67.066203.

[14] Sergey Bravyi, David P. DiVincenzo, and Daniel Loss. Schrieffer–Wolff transformation for quantum many-body systems. *Annals of Physics*, 326:2793–2826, 2011. doi: 10.1016/j.aop.2011.06.004.

[15] Chiara Marletto and Vlatko Vedral. Evolution without evolution, and without ambiguities. *Physical Review D*, 95:043510, 2017. doi: 10.1103/PhysRevD.95.043510.

[16] Alexander R. H. Smith and Mehdi Ahmadi. Quantizing time: Interacting clocks and systems. *Quantum*, 3:160, 2019. doi: 10.22331/q-2019-07-08-160.

[17] Esteban Castro Ruiz, Flaminia Giacomini, and Časlav Brukner. Entanglement of quantum clocks through gravity. *Proceedings of the National Academy of Sciences*, 114:E2303, 2017. doi: 10.1073/pnas.1616427114.

[18] Ashmeet Singh and Oliver Friedrich. Emergence of Gravitational Potential and Time Dilation from Non-interacting Systems Coupled to a Global Quantum Clock. *Foundations of Physics*, 55:82, 2025. doi: 10.1007/s10701-025-00893-8.

[19] Dario Cafasso, Nicola Pranzini, Jorge Yago Malo, Vittorio Giovannetti, and Marilù Chiofalo. Quantum time and the time-dilation induced interaction transfer mechanism. *Physical Review D*, 110:106014, 2024. doi: 10.1103/PhysRevD.110.106014.

[20] Tommaso Favalli. *On the Emergence of Time and Space in Closed Quantum Systems*. Springer Theses. Springer, 2024. doi: 10.1007/978-3-031-52352-6.

[21] Magdalena Zych and Časlav Brukner. Quantum formulation of the Einstein equivalence principle. *Nature Physics*, 14:1027–1031, 2018. doi: 10.1038/s41567-018-0197-6.

[22] Steven Weinberg. Photons and gravitons in S-matrix theory: Derivation of charge conservation and equality of gravitational and inertial mass. *Physical Review*, 135:B1049, 1964. doi: 10.1103/PhysRev.135.B1049.

[23] David Elliman. Supporting code and evidence for relational clocks in a quantum ledger, 2026. URL `https://doi.org/10.5281/zenodo.24109717`. Version 1.0.0. Concept DOI: 10.5281/zenodo.24109716. The URL above identifies the exact version.